

# A Synchrotron SAXS Study of Miscible Blends of Semicrystalline Poly(vinylidene fluoride) and Semicrystalline Poly(1,4-butylene adipate)

Li-Zhi Liu and Benjamin Chu\*

Department of Chemistry, State University of New York at Stony Brook,  
Stony Brook, Long Island, New York 11794-3400

J. P. Penning† and R. St. John Manley

Department of Chemistry, McGill University, 3420 University Street,  
Montreal, Quebec, Canada H3A 2A7

Received November 22, 1996; Revised Manuscript Received April 10, 1997®

**ABSTRACT:** The morphology of a miscible blend of two crystalline polymers (PVF<sub>2</sub>/PBA) has been investigated by synchrotron small-angle X-ray scattering. Measurements have been made as a function of blend composition and of temperature, probing the morphologies at both the spherulitic and the lamellar levels in both the semicrystalline/semicrystalline and the semicrystalline/amorphous states. The correlation function analysis of SAXS profiles has permitted the determination of characteristic morphological parameters at the lamellar level. For the semicrystalline/amorphous state of the blends containing up to 50 wt % of PBA, the amorphous PBA was (mainly) incorporated between the crystalline PVF<sub>2</sub> lamellae, i.e. in the interlamellar region. In the case of semicrystalline/semicrystalline blends, the morphology was more complex. In addition to the pronounced scattering peak from the PVF<sub>2</sub> crystalline lamellae, there was a scattering shoulder (or small peak) related to the PBA crystals, indicating that the PVF<sub>2</sub> and PBA lamellae were in a segregated arrangement. Taken together, the data led us to the conclusion that PBA could crystallize as a thick lamella in the PVF<sub>2</sub> interlamellar region and that there was a mixed amorphous phase on either side of the PBA lamella, i.e. between the PBA and PVF<sub>2</sub> crystal lamellae. The proposed structure model for the semicrystalline/semicrystalline PVF<sub>2</sub>/PBA blends is different from the model proposed by Cheung *et al.* (Macromolecules 1994, 27, 2520) for semicrystalline/semicrystalline (PCL/PC) blends whereby a random mixture of PC and PCL lamellae exist.

## Introduction

Semicrystalline/semicrystalline blends can exhibit a complicated phase behavior, including semicrystalline/amorphous and semicrystalline/semicrystalline states. At a temperature between the melting points,  $T_m$ s, of the two components, the blend is actually a semicrystalline/amorphous system, and the amorphous component can reside between the crystalline lamellae (interlamellar),<sup>1,2</sup> can be incorporated within the spherulites (interfibrillar),<sup>3</sup> or can even be rejected from the spherulites (interspherulitic).<sup>4</sup> In the semicrystalline/semicrystalline state, the blend can exhibit much more complex morphologies. Cheung *et al.*<sup>5,6</sup> recently studied the phase behavior and morphologies of a semicrystalline/semicrystalline miscible blend of polycarbonate (PC) and poly( $\epsilon$ -caprolactone) (PCL). In the semicrystalline/amorphous state (above the melting point of PCL), it was found that, with addition of PCL, PCL was incorporated into the amorphous phase between the crystalline lamellae in the PC-rich blends, as shown by an increase in the amorphous-phase thickness, whereas the crystal phase thickness remained fairly constant. PCL was rejected from the PC interlamellar region in the PCL-rich blends, as indicated by the invariance of the long period and the amorphous phase thickness with composition. Since there is a large difference between the glass transition temperatures,  $T_g$ , of PC ( $\sim 150$  °C) and PCL ( $\sim -50$  °C), the  $T_g$  of the blend changes appreciably with blend composition, especially in the PC-rich blend,<sup>5</sup> with the result that only the blends

containing >30 wt % of PCL have glass transition temperatures below room temperature. The transition from interlamellar inclusion to interlamellar exclusion was postulated to be related to the glass transition temperatures or the mobility of the blends. The PC/PCL blends showed only one small-angle scattering peak (SAXS) both in the semicrystalline/amorphous state and in the semicrystalline/semicrystalline state. The SAXS profiles were interpreted in terms of scattering from entities composed of a random mixture of PC and PCL lamellae in the semicrystalline/semicrystalline state.

In the PC/PCL blends, the low- $T_m$  component (PCL) cannot crystallize in most of the blends rich in the high- $T_m$  component (PC), due to the high  $T_g$ s of the blends resulting from the much higher  $T_g$  of PC than that of PCL. As a result, the study of the crystallization behavior and morphologies of the semicrystalline/semicrystalline PC/PCL system was limited mainly to the blends rich in the low- $T_m$  component (PCL). Very recently, another semicrystalline/semicrystalline miscible blend system of poly(vinylidene fluoride) (PVF<sub>2</sub>) and poly(1,4-butylene adipate) (PBA) was studied by us, including the miscibility, the phase behavior, the crystallization behavior, and the spherulitic morphologies.<sup>7–9</sup> In the PVF<sub>2</sub>/PBA system, the  $T_g$  of the blend changes only slightly with blend composition because the glass transition temperatures<sup>7</sup> of PVF<sub>2</sub> ( $\sim -43$  °C) and PBA ( $\sim -60$  °C) are quite close. The weak  $T_g$  dependence of the PVF<sub>2</sub>/PBA blend on blend composition offers two advantages: first, both PVF<sub>2</sub> and PBA readily crystallize from their mixtures over a wide range of composition, and thus the crystallization and morphology of the blends composed mainly of a high- $T_m$  component (PVF<sub>2</sub>

\* Author to whom correspondence should be addressed.

† Present address: Akzo Nobel Central Research, Department RDS, P.O. Box 9300, 6800 SB Arnhem, The Netherlands.

® Abstract published in *Advance ACS Abstracts*, June 15, 1997.

in our case) can also be investigated; second, it is a good system to investigate whether the transition from interlamellar inclusion to interlamellar exclusion is related to the change in glass transition temperature with blend composition. Another difference in the SAXS behavior between the PVF<sub>2</sub>/PBA and PC/PCL blend systems is that only one scattering peak was observed for the PC/PCL system, while two scattering peaks (or one peak and one shoulder) were observed in our system in the semicrystalline/semicrystalline state. The results for the PVF<sub>2</sub>/PBA system suggest a new lamellar organization model in which a PBA lamella is formed in the PVF<sub>2</sub> interlamellar phase as the PBA content is increased. The experimental evidence is indicated by an increase in the thickness of the PVF<sub>2</sub> interlamellar phase and by the presence of another SAXS scattering peak which disappears above the melting point of PBA. In the present paper, we describe a study of the morphology of miscible PVF<sub>2</sub>/PBA blends at the lamellar level in both the semicrystalline/semicrystalline state and the semicrystalline/amorphous state.

### Experimental Section

**Materials.** The PVF<sub>2</sub> ( $M_w = 1.4 \times 10^5$ ) sample used in this study was supplied by Polysciences Inc. (Warrington, PA) and was used as received. The PBA sample was obtained from Scientific Polymer Products, Inc. (Ontario, NY) and was purified by reprecipitation from *N,N*-dimethylformamide (DMF) into cold methanol ( $-10^\circ\text{C}$ ). The weight average and number average molecular weights of the as-precipitated PBA were  $1.4 \times 10^4$  and  $9.8 \times 10^3$ , respectively, as determined by gel permeation chromatography using 1,4-dioxane as the eluent.

Blends of PVF<sub>2</sub> and PBA were prepared by solvent casting using DMF as a mutual solvent. Stock solutions of both polymers (initial concentration 2 g/100 mL) were mixed in the desired proportions, well stirred, and subsequently cast onto Teflon dishes. The solvent was allowed to evaporate in a controlled air stream for 24 h, and the resulting films were further dried in vacuum at room temperature for 3 days. In this way, blends were prepared with various compositions ranging from 90/10 to 40/60 in a ratio of weight percent, the first numeral referring to PVF<sub>2</sub>. The samples thus prepared were compression molded at  $190^\circ\text{C}$  and then quenched from this temperature to room temperature ( $\sim 20^\circ\text{C}$ ) in a water bath.

**Synchrotron Small-Angle X-ray Scattering (SAXS).** The scattering experiments were performed at the SUNY X3-A2 beamline of the National Synchrotron Light Source (NSLS), Brookhaven National Laboratory (BNL). The X-ray wavelength used was 0.154 nm. A laser-aided prealigned pinhole collimation system<sup>10</sup> was utilized with a sample to detector distance of 1065 mm. Small angles down to 1.5 mrad corresponding to a  $d$ -spacing ( $d = 2\pi/q_{\min}$ ) of about 100 nm have been achieved. Fuji imaging plates were used to collect the scattering data with exposure times of 2 min per frame. The scattering profiles were corrected for sample absorption, background, and incident X-ray intensity fluctuations.

### Results and Discussion

On the basis of thermal analysis results, the PVF<sub>2</sub>/PBA blend is miscible in the amorphous phase over the entire composition range, as evidenced by the presence of a single glass transition temperature and a melting point depression.<sup>7</sup> In the melt state,  $\sim 60^\circ\text{C}$  above the melting temperature of the PVF<sub>2</sub>, a thermally reversible lower critical solution temperature (LCST) was observed. A one-phase region is located between the PVF<sub>2</sub> liquidus and the cloud-point curve. Lowering the temperature to  $T_m(\text{PVF}_2) > T > T_m(\text{PBA})$  will cause the PVF<sub>2</sub> component to crystallize and thus to segregate from the mixture. In this temperature regime, the

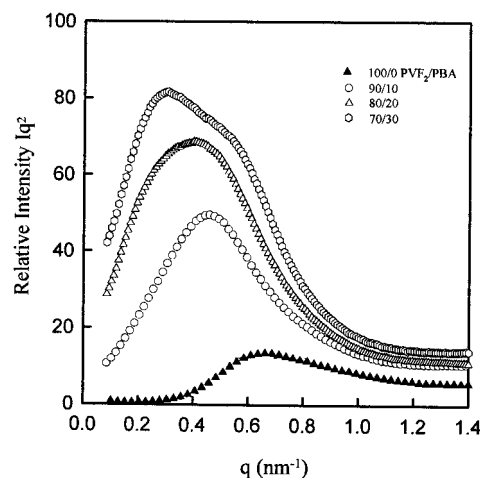


**Figure 1.** Lorentz-corrected SAXS profiles of the PVF<sub>2</sub> homopolymer and its blends with 10–30 wt % PBA in the semicrystalline/semicrystalline state ( $\sim 20^\circ\text{C}$ ).

blends are semicrystalline/amorphous. Further lowering of the temperature to  $T < T_m(\text{PBA})$  will induce crystallization of the PBA component, leading to a three-phase morphology in which two distinct crystalline phases coexist with a mixed amorphous phase. Differential scanning calorimetry (DSC) measurements show that when the blend is cooled from the melt at a cooling rate of  $20^\circ\text{C}/\text{min}$ , the crystallization temperature,  $T_c$ , of PVF<sub>2</sub>, which corresponds to the peak position of the crystallization exotherm, is about  $70^\circ\text{C}$  higher than that of the PBA of the blend, showing that the two polymers crystallize in different, well-separated temperature regimes. It was also concluded that crystallization of PVF<sub>2</sub> is always complete before crystallization of PBA commences, even at a very fast cooling rate of  $200^\circ\text{C}/\text{min}$  from the melt.<sup>8</sup> In the present work, the samples were quenched from the melt ( $190^\circ\text{C}$ ) directly to room temperature ( $\sim 20^\circ\text{C}$ ) at an estimated rate of  $200^\circ\text{C}/\text{min}$ . A time-resolved SAXS study<sup>11</sup> showed that when the blend was quenched from  $190^\circ\text{C}$  directly to room temperature, the crystallization of PVF<sub>2</sub> and of PBA remained as two separated processes; i.e., when the blend is cooled from the amorphous single phase to room temperature, PVF<sub>2</sub> crystallizes first and proceeds through free growth of spherulites from the homogeneous melt. The PBA component acts as a noncrystalline diluent during the crystallization of the PVF<sub>2</sub> component and starts to crystallize later in the miscible mixed region of PBA and amorphous PVF<sub>2</sub>. The three-phase structures of the miscible PVF<sub>2</sub>/PBA blends quenched from  $190^\circ\text{C}$  to room temperature and the two-phase structure after heating the blends to above the melting point of PBA were studied by using the synchrotron SAXS technique.

**1. Scattering Behavior of PVF<sub>2</sub>/PBA Blends in the Two-Phase and Three-Phase States.** Scattering profiles for the PVF<sub>2</sub>/PBA blends at various compositions are shown in Figures 1 and 2. The pure PVF<sub>2</sub> homopolymer exhibits a broad scattering peak, while the pure PBA homopolymer exhibits a sharp scattering peak, indicating that the packing of the lamellar stacks in PBA is more regular than that in PVF<sub>2</sub>. By comparing the scattering curves of the blends and the corresponding homopolymers, it is seen from Figures 1 and 2 that the scattered intensity of the blends is much higher than that of the homopolymers and increases enormously with increasing PBA content. Since the PBA density ( $\rho = 1.23 \text{ g}/\text{cm}^3$ ) is much smaller than that

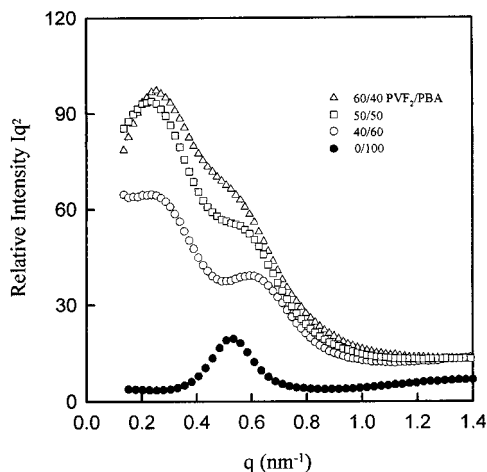


**Figure 2.** Lorentz-corrected SAXS profiles of the PBA homopolymer and the PVF<sub>2</sub>/PBA blends with 40–60 wt % PBA in the semicrystalline/semicrystalline state ( $\sim 20^\circ\text{C}$ ).

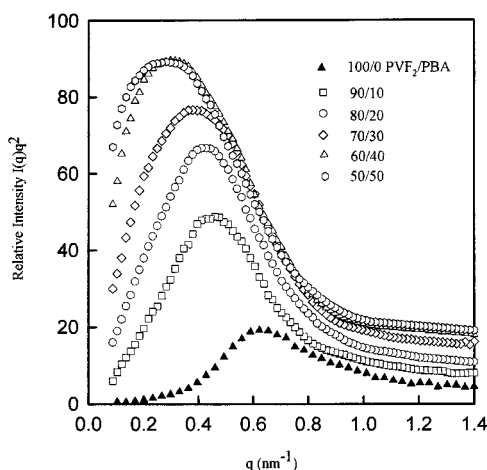


**Figure 3.** Lorentz-corrected SAXS profiles of the PVF<sub>2</sub> homopolymer and its blends with 10–50 wt % PBA in the semicrystalline/amorphous state ( $70^\circ\text{C}$ ).

of PVF<sub>2</sub> ( $\rho = 1.80\text{ g/cm}^3$ ), the incorporation of PBA into the PVF<sub>2</sub> interlamellar region could cause a much larger density difference between the crystallized PVF<sub>2</sub> lamella and the interlamellar region, which could, in turn, result in a much stronger SAXS scattering.

The position of the scattering peak from the blend shifts to a lower scattering angle with increasing PBA content, as shown in Figure 1 for the 90/10 and 80/20 blends. A scattering shoulder begins to appear at the high- $q$  range of the scattering peak with a further increase in the PBA weight fraction, as also seen in Figure 1 for the 70/30 blend. This scattering shoulder at  $q \sim 0.5\text{ nm}^{-1}$  becomes prominent with a further increase in the PBA content. In particular, a clear scattering shoulder is observed for the 60/40 blend, and finally it appears as a well-defined peak for the 40/60 blend, as shown in Figure 2. The dependence of the scattering shoulder (or peak) on the PBA weight fraction suggests that it could be related to the PBA scattering in the semicrystalline/semicrystalline state. To confirm the supposition on the origin of the scattering shoulder (or peak), SAXS measurements of the blends were also conducted at  $70^\circ\text{C}$ , which is above the melting point of PBA. As shown in Figure 3, the scattering shoulder (or peak) at the high- $q$  range disappears for all the blends at  $70^\circ\text{C}$ . The absence of this scattering shoulder (or peak) above the melting point of PBA confirms that the

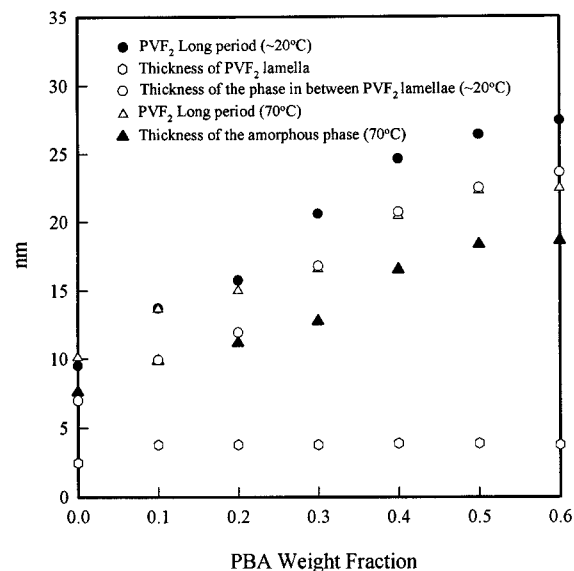


**Figure 4.** Long period of PVF<sub>2</sub> in the blend, as determined from the peak position of the Lorentz-corrected SAXS curve; the average thickness of the PVF<sub>2</sub> lamellae and the average thickness of the phase in between the PVF<sub>2</sub> lamellae versus weight fraction of PBA.

scattering shoulder (or peak) is related to the scattering from the PBA component.

**2. Crystalline Structure of PVF<sub>2</sub> and Spatial Distribution of PBA in the Two-Phase State.** As discussed above, the PVF<sub>2</sub> lamellar stacks showed a scattering peak in both the two-phase and the three-phase states. The long period or the interlamellar spacing of the PVF<sub>2</sub> in the blend was calculated from the equation  $L = 2\pi/q^*$ , where  $q^*$  is the peak value found in the Lorentz-corrected SAXS ( $q^2 I(q)$  versus  $q$ ) plot or the first peak value in the low- $q$  range for the two observed peaks (or shoulders). As shown in Figure 4, the long period of PVF<sub>2</sub> in the blend at room temperature increases nearly linearly with increasing PBA content up to 50 wt %. The long period of the pure PVF<sub>2</sub> homopolymer (filled circle with PBA weight fraction equal to zero) is 9.5 nm, while the long period of the 50/50 blend is increased to 26.4 nm (filled circle with PBA weight fraction equal to 0.5), about 2.8 times larger than that of the pure PVF<sub>2</sub> homopolymer. By further increasing the PBA weight fraction of the blend, the PVF<sub>2</sub> long period remained almost unchanged, as shown in Figure 4. The increase in the long period of PVF<sub>2</sub> with increasing PBA content was also observed when the blend was heated to above the melting point of PBA, as shown by hollow triangles in Figure 4. However, the blends with 30 wt % PBA or more, which exhibited a scattering shoulder (or peak) on the higher  $q$  side of the scattering peak of PVF<sub>2</sub> lamellae, show an appreciably smaller long period of PVF<sub>2</sub> at the PBA melt state ( $70^\circ\text{C}$ ) compared with that at room temperature ( $20^\circ\text{C}$ ).

In the semicrystalline/amorphous state, only the PVF<sub>2</sub> component could be crystallized, and the PBA component is incorporated into the interlamellar, interfibrillar, and/or interspherulitic regions. To investigate the PVF<sub>2</sub> morphology at the lamellar level and the PBA spatial distribution in the blend, the average PVF<sub>2</sub> crystalline-phase thickness and the average amorphous-phase (composed of amorphous PVF<sub>2</sub> and PBA) thickness of the blend in the semicrystalline/amorphous state were calculated from the normalized one-dimensional correlation function  $\gamma(z)$ , evaluated from the scattered intensity  $I(q)$  by the following equation:<sup>12</sup>

$$\gamma(z) = (1/\gamma(0)) \int_0^\infty q^2 I(q) \cos(qz) dq$$

where  $z$  is the correlation distance along the direction from which the electron density distribution is measured. As the experimentally accessible  $q$  range is finite, it was necessary to extend the data to both lower and higher  $q$  values. The intensity versus  $q$  data were linearly extrapolated from the smallest measured  $q$  value to zero. Large  $q$  values were damped to infinite  $q$  by using the Porod–Ruland theory.<sup>13–14</sup> In fact, we have used two additional methods for an extrapolation to low  $q$ : the extrapolation based on the Guinier law and the extrapolation by using the Debye–Bueche model.<sup>15</sup> The results show that the three different extrapolation methods to low  $q$  values make no observable difference to our findings. The same values were obtained with different extrapolation methods. It is noted that the lowest  $q$  values we were able to achieve were less than  $0.08 \text{ nm}^{-1}$ , making the extrapolation method less critical, and that the scattering peak position, as seen in the Lorentz-corrected SAXS curves (Figure 3), was sufficiently far away from the low- $q$  values, also making the extrapolation method less critical. Figure 5 shows a typical correlation function of pure PVF<sub>2</sub>, demonstrating how the long period  $L$ , the crystalline-phase thickness  $C$ , and the amorphous phase thickness  $A (=L - C)$  can be estimated from the correlation function curve. In addition to the scattering peak, which is related to the PVF<sub>2</sub> lamellae shown in Figures 1 and 2, most SAXS profiles of the blends have another scattering peak or shoulder related to the PBA crystals. In this case, the long period of the PVF<sub>2</sub> in the blend can still be calculated from the equation  $L = 2\pi/q^*$ . However, it is no longer easily obtained from the correlation function analysis because of the complexity in the correlation function curve caused by the presence of another scattering peak or shoulder related to the PBA crystals. Therefore, in order to compare the morphology of the blends at room temperature with that above the melting point of the PBA component at the lamellar level, the average thickness of the PVF<sub>2</sub> interlamellar phase ( $A = L - C$ ) was calculated by using the  $C$  value obtained from the correlation function analysis and the  $L$  value derived from the Lorentz-corrected SAXS plot ( $L = 2\pi/q^*$ ). In fact, the long period of the PVF<sub>2</sub> homopolymer derived from  $L = 2\pi/q^*$  is equal to 9.5 nm, in good agreement with that shown by the maximum peak position of the correlation function curve of the homopolymer, as shown in Figure 5.

In Figure 4, the average crystalline phase thickness  $C$  (hollow hexagons) of the quenched PVF<sub>2</sub> homopolymer at 70 °C was about 2.5 nm. With the addition of 10 wt % PBA, the thickness was increased to about 3.8 nm, and it remained almost unchanged with further addition of PBA. This experimental observation is different from the reported results for PC/PCL blends in the semicrystalline/amorphous state, where the PC crystalline-phase thickness decreased with increasing PCL content,<sup>6</sup> and the results from the miscible semicrystalline/amorphous blends of poly(ethylene oxide) (PEO) and poly(methyl methacrylate) (PMMA), where most of the blends showed a smaller crystalline-phase thickness than that of the pure PEO.<sup>2</sup> The larger crystalline-phase thickness of the PVF<sub>2</sub>/PBA blend when compared with that of the pure PVF<sub>2</sub> homopolymer was also observed in the time-resolved SAXS study of the isothermal crystallization of the 40/60 blend and of the pure PVF<sub>2</sub> homopolymer at 130 °C.<sup>11</sup> The difference in the dependence of the

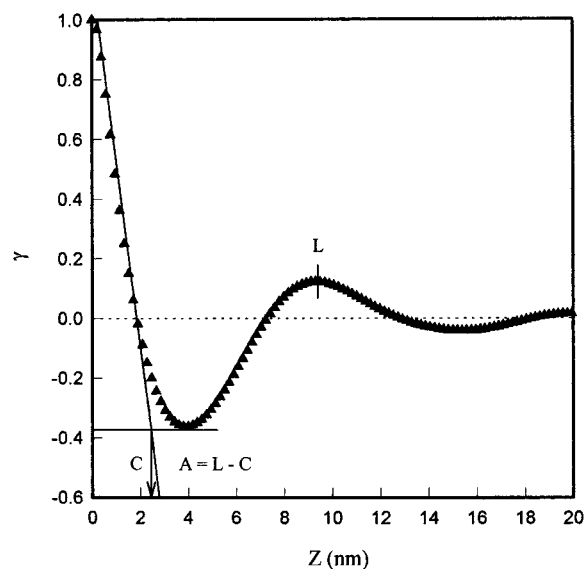


**Figure 5.** Correlation function of the pure PVF<sub>2</sub> homopolymer with  $L$  = long period,  $C$  = crystalline-phase thickness, and  $A$  = amorphous-phase thickness ( $L - C$ ).

crystalline-phase thickness on blend composition for different blend systems is probably related to the glass transition behavior of the blends. The  $T_g$  of PC/PCL and of PVF<sub>2</sub>/PBA blends decreases with addition of the low- $T_m$  component (PCL or PBA), which is an amorphous component in the semicrystalline/amorphous state, while the  $T_g$  of the PEO/PMMA blend increases with addition of the amorphous component (PMMA). PC is normally classified as an amorphous polymer due to its very low crystallinity. In the PC/PCL blend, however, the lower  $T_g$  of the blend than that of the pure PC induces a much higher crystallinity of the PC component in the blend than that of the pure PC homopolymer.<sup>6</sup> Thus, the PC in the blend could readily undergo crystallization even at room temperatures.<sup>16</sup> For the PVF<sub>2</sub>/PBA blend, it was also observed that the PVF<sub>2</sub> crystallinity in the blend was much higher than that of the pure PVF<sub>2</sub> homopolymer, probably because the  $T_g$  of the blend was lower than that of the PVF<sub>2</sub> homopolymer.<sup>7</sup> The appreciably larger crystalline-phase thickness of PVF<sub>2</sub> in the blend than that in the pure PVF<sub>2</sub> homopolymer could presumably also have resulted from the lower  $T_g$  of the blend when compared with that of PVF<sub>2</sub> homopolymer. The observed smaller, instead of larger, crystalline-phase thickness of the PC component in the PC/PCL blend when compared with that of the PC homopolymer<sup>6</sup> was probably due to the weak PC crystallizability.

The lamellar organization of PVF<sub>2</sub> in the blend may also be changed with PBA content. Figure 6 shows the original SAXS profiles ( $I(q) \sim q$ ) of some of the blends, as well as those of PVF<sub>2</sub> and PBA homopolymers. The PVF<sub>2</sub> homopolymer shows a clear broad scattering peak near  $q \sim 0.6 \text{ nm}^{-1}$ . However, the 90/10 blend exhibited only a scattering shoulder, and the 80/20 blend merely showed a scattering decay. This appreciable change in scattering behavior with addition of a limited amount of the PBA homopolymer may be explained as follows. The presence of the PBA homopolymer reduced the PVF<sub>2</sub> lamellar stacks, when compared with those of the pure PVF<sub>2</sub> homopolymer. The peak width ( $\beta$ ) measured at half-height of the Lorentz-corrected SAXS profiles is

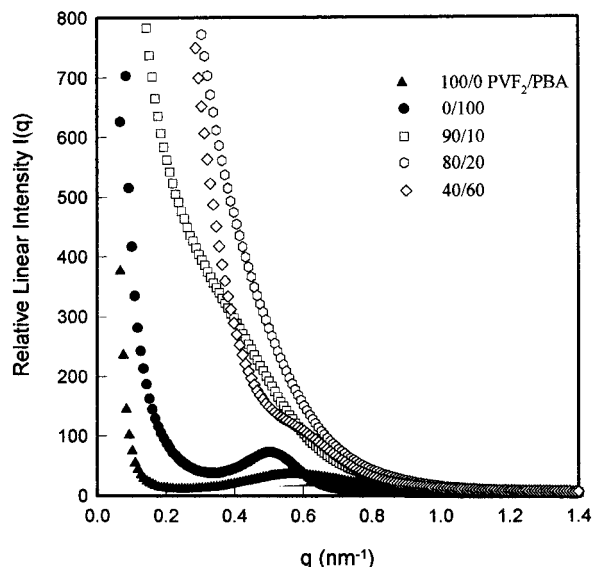


**Figure 6.** Linear SAXS profiles of the PBA and PVF<sub>2</sub> homopolymers as well as some of the PVF<sub>2</sub>/PBA blends in the semicrystalline/semicrystalline state ( $\sim 20^\circ\text{C}$ ).

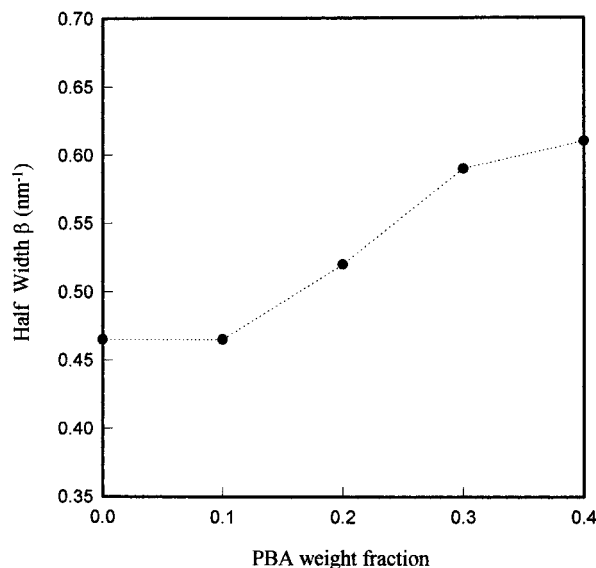


**Figure 7.** Scattering peak width at half-height of the blends with  $\leq 40$  wt % PBA in the semicrystalline/amorphous state ( $70^\circ\text{C}$ ).

usually used as a measure of the homogeneity of the lamellar distribution. Figure 7 shows a plot of the peak width as a function of composition for the blends in the semicrystalline/amorphous state ( $70^\circ\text{C}$ ). The  $\beta$  value of the blend with 10 wt % PBA was almost the same as that of the PVF<sub>2</sub> homopolymer. Then  $\beta$  was increased sharply with further addition of PBA. This change in peak width at half height with blend composition suggests that the PVF<sub>2</sub> lamellar heterogeneity has increased significantly for the blend with 20 or more wt % PBA.

The thickness of the amorphous phase for the blend at  $70^\circ\text{C}$  (filled triangles in Figure 4) and the thickness of the phase in between the PVF<sub>2</sub> crystalline lamellae at room temperature (hollow circles in Figure 4) were calculated in terms of the average thickness of the PVF<sub>2</sub> crystalline lamellae (hollow hexagons in Figure 4), obtained from the correlation function analysis of the SAXS data at  $70^\circ\text{C}$ , and the PVF<sub>2</sub> long period at the corresponding temperatures (hollow triangles or filled circles in Figure 4). The amorphous-phase thickness

of the blend at  $70^\circ\text{C}$  increased approximately linearly with addition of PBA, up to 50 wt % PBA. The considerable increase in the average thickness of the amorphous phase, and the large increase in the scattered intensity with increasing PBA content mentioned above, suggest that the PBA homopolymer is mainly sandwiched in between the PVF<sub>2</sub> crystalline lamellae for the blends containing up to 50 wt % PBA. By further increasing the PBA weight fraction, the amorphous-phase thickness remained nearly constant, indicating that the additional PBA could be located mainly in the interfibrillar region or in both the interfibrillar and the interspherulitic regions.

A previous study<sup>8</sup> of the radial growth rates of PVF<sub>2</sub> in various blends containing up to 80 wt % PBA showed that, for the blends containing up to 50 wt % PBA, the spherulite radius  $R$  increased linearly with time up to the point of impingement, implying a constant growth rate throughout the crystallization process. The linear growth rate in  $R$  suggests that the PBA molecules, which were rejected from the growing PVF<sub>2</sub> crystals, did not migrate away from the spherulitic growth front but rather became trapped within the interlamellar and interfibrillar regions of the growing spherulites. In the blends containing 60 or more wt % PBA, a nonlinear growth rate of the spherulites was observed at the advanced stages of crystallization, indicating that in this case the noncrystalline material accumulated, to a certain extent, in the interspherulitic domains. The crystallization of PBA from the blend containing 60 wt % PBA was also directly observed in the interspherulitic domains of the pre-existing PVF<sub>2</sub> morphology by optical microscopy.<sup>8</sup> The conclusions about the distribution of the PBA component in the blend, reached by the previous study of the radial growth rates of PVF<sub>2</sub> spherulites, are consistent with the conclusions reached here by the analysis of the morphology at the lamellar level.

A time-resolved SAXS study<sup>11</sup> of the blends has shown the following behavior. Starting from the semicrystalline/amorphous state, which was reached by isothermally crystallizing PVF<sub>2</sub> at  $130^\circ\text{C}$ , and then quenching the blend to room temperature so that PBA began to crystallize, the long period of PVF<sub>2</sub> decreased with time, due to a decrease in the volume of the PVF<sub>2</sub> interlamellar region as the PBA was crystallized. By returning to the semicrystalline/amorphous state, the long period of the PVF<sub>2</sub> in the blend should increase to the value that it had before quenching to room temperature. In the present work, the samples were prepared by quenching from a single phase directly to the three-phase region. However, when the blend was heated back to the semicrystalline/amorphous state (at  $70^\circ\text{C}$ ), an appreciable decrease in the long period of PVF<sub>2</sub> (hollow triangles in Figure 4) was observed for the blend with 30 or more wt % PBA, when compared with the long period of the blend before heating (filled circles in Figure 4). The thickness of the PVF<sub>2</sub> crystalline phase in the blend is supposed to be the same both at room temperature and at  $70^\circ\text{C}$ , so the change in the PVF<sub>2</sub> long period must come from the change in the PVF<sub>2</sub> interlamellar region. The considerable decrease of the PVF<sub>2</sub> long period in the blend at  $70^\circ\text{C}$  implies that the thickness of the phase located in between the PVF<sub>2</sub> lamellae is smaller than that of the blend at room temperature ( $\sim 20^\circ\text{C}$ ). This decrease in the PVF<sub>2</sub> long period at  $70^\circ\text{C}$  indicates that part of the PBA in the PVF<sub>2</sub> interlamellar region diffused into the interfibrillar

region and possibly even into interspherulitic regions. Meanwhile, the amorphous-phase thickness still showed an appreciable increase with increasing PBA weight fraction (up to 0.5). The above two features about the PVF<sub>2</sub> long period and the amorphous-phase thickness at 70 °C suggest that, with an increase of the amorphous component in the miscible semicrystalline/amorphous blends, the amorphous component is incorporated partly in the interlamellar region, resulting in an increase in the thickness of the amorphous phase, and partly in the interfibrillar region. As shown in Figure 4, when the blends were heated back to 70 °C, the thickness of the PVF<sub>2</sub> interlamellar phase shows no change for the 90/10 blend, a small decrease for the 80/20 blend, and a considerable decrease for the blends with 30 wt % or more PBA. This suggests that the ratio of the PBA component incorporated in the interlamellar region to that in the interfibrillar region decreases when the amorphous component increases, which eventually results in the transition from interlamellar inclusion to the interlamellar exclusion. It is also possible that after the thickness of the PVF<sub>2</sub> interlamellar phase approached a constant value, any additional PBA could be incorporated partly in the interfibrillar region and partly in the interspherulitic region. In contrast to the case of PC/PCL blends,<sup>5,6</sup> the transition from (mainly) interlamellar inclusion to interlamellar exclusion is probably not related to the change in the glass transition temperature with blend composition because the  $T_g$  of the PVF<sub>2</sub>/PBA blends changes only slightly with composition.

**3. Crystalline Structure of PBA under the Influence of the Partially Solidified PVF<sub>2</sub> Phase.** When the PVF<sub>2</sub>/PBA blends containing less than 50 wt % PBA were quenched from 190 °C to room temperature, the PBA component was mainly incorporated in between the PVF<sub>2</sub> crystalline phase, and PBA started to crystallize after completion of the crystallization of the PVF<sub>2</sub> phase. The crystallization of PBA is physically constrained by the spherulitic microstructure of the PVF<sub>2</sub> crystalline phase. In addition, the crystallinity of PBA decreased rapidly with decreasing PBA weight fraction in the blend, and only in the blends containing 20 wt % or more PBA does PBA crystallize readily.<sup>7</sup> The confined region for the crystallization of PBA and the weaker crystallizability of PBA due to its miscibility with PVF<sub>2</sub> might result in very different crystalline structures of PBA in the blend than in the pure PBA homopolymer. As shown in Figure 8, the SAXS profile of the 90/10 blend at room temperature is almost the same as that above the  $T_m$  of PBA. The SAXS profile suggests that the PBA was unable to crystallize in this blend, which is consistent with the previous conclusion reached by the DSC study.<sup>7</sup> However, the 80/20 blend gave a sharper SAXS peak for the melt state of PBA than that at room temperature, as shown in Figure 8. The peak width at half height at room temperature was 0.60 nm<sup>-1</sup>, while it decreased to 0.52 nm<sup>-1</sup> at 70 °C. The broader peak of the 80/20 blend at room temperature suggests that the PBA component is partially crystallized in this blend. The scattering of PBA crystals in the 80/20 blend is located at the lower  $q$  range of the scattering peak. The scattering behavior of the PBA in the 80/20 blend suggests that the PBA is crystallized into many microcrystals in between the PVF<sub>2</sub> lamellae and that the average interdistance of the PBA microcrystals is larger than the average long period of the PVF<sub>2</sub> in the blend. The interdomain distance of

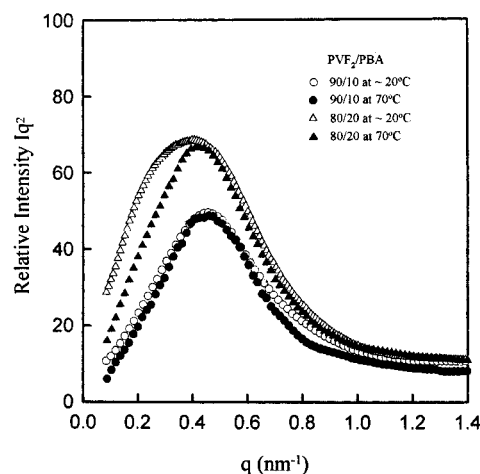


**Figure 8.** Comparison of Lorentz-corrected SAXS profiles of blends with 10–20 wt % PBA in the semicrystalline/amorphous state (70 °C) and the semicrystalline/semicrystalline state (~20 °C).

PBA crystals in the 80/20 blend (~20.9 nm, estimated from the PBA scattering around  $q = 0.3 \text{ nm}^{-1}$ ) is also much larger than the long period of the pure PBA homopolymer (11.9 nm), and the larger interdistance is presumably due to the very low crystallinity of the PBA in this blend<sup>7</sup> and the existence of the amorphous PVF<sub>2</sub> among the PBA crystals. As the weight fraction of PBA in the blend was increased to 0.3, a scattering shoulder started to appear in the higher  $q$  range of the scattering peak, as shown in Figure 1. This scattering shoulder could be related to the scattering of the PBA component, discussed in the last section, by its disappearance above the melting point of PBA. The scattering shoulder might also be the result of small PBA crystals formed in between the PVF<sub>2</sub> lamellae. The scattering shoulder related to PBA crystals in the 70/30 blend appeared at a higher  $q$  range ( $q = \sim 0.55 \text{ nm}^{-1}$ ) than the scattering contribution of the PBA microcrystals in the 80/20 blend ( $q = \sim 0.3 \text{ nm}^{-1}$ ), indicating that the interdomain distance of the PBA crystals in the 70/30 blend became much smaller than that in the 80/20 blend. The fact that the  $q$  position of the scattering shoulder of the 70/30 blend was almost the same as that of the scattering peak of the pure PBA homopolymer (Figure 2) suggested that the separation distance of the PBA microcrystals in the 70/30 blend was already close to the long period in the pure PBA homopolymer. Therefore, it could be expected that, with a further increase in the PBA content in the blend, a thick PBA lamella could be formed in the PVF<sub>2</sub> interlamellar phase.

As can be seen from Figure 2, by further increasing the PBA weight fraction to 0.5, the scattering shoulder became more pronounced; i.e., a clear scattering shoulder was observed. It is possible that the PBA component may have crystallized as a thick lamella right in between the PVF<sub>2</sub> crystalline lamellae, and two miscible amorphous phases of PBA and PVF<sub>2</sub> are formed on both sides of the PBA lamella, i.e. in between the PBA and PVF<sub>2</sub> crystalline lamellae. A study<sup>7</sup> of the equilibrium melting point of PBA in the blends containing 40 wt % or more PBA showed that the  $T_m$  was almost the same as that of pure PBA, indicating that the PBA in the 60/40 and 50/50 blends could still form lamellae similar to those of the pure PBA homopolymer. That is, the PBA in the 60/40 and 50/50 blends could more likely form thick lamellae in between the PVF<sub>2</sub> lamellae rather

than many smaller crystals, and the PBA lamellae formed in the blends are expected to have approximately the same thickness as the crystalline lamellae in the pure PBA homopolymer. The scattering shoulder might correspond to the coherent scattering of the mixed amorphous phase of PBA and PVF<sub>2</sub> in between the PVF<sub>2</sub> crystalline lamellae and the PBA crystalline lamellae. It is noted that the thickness of the PVF<sub>2</sub> interlamellar region of the blend containing 20 wt % PBA was 11.9 nm, which is the same as the long period of the PBA homopolymer (11.9 nm) crystallized under the same quenching conditions. However, no scattering peak or shoulder related to the PBA crystals was observed. The thickness of the PVF<sub>2</sub> interlamellar region of the blend containing 50 wt % PBA was 22.5 nm (Figure 4), which is only about 1.9 times the long period of the PBA homopolymer (11.9 nm) crystallized under the same quenching conditions. Therefore, no more than one thick PBA lamella could be formed in the PVF<sub>2</sub> interlamellar phase, because of the limited thickness of the interlamellar phase and of the equivalent PBA crystal size in the blend and in the pure PBA homopolymer. By further increasing the PBA weight fraction of the blend to 0.6, the scattering shoulder, as observed for the 60/40 and 50/50 blends, changed into a peak, as shown in Figure 2. The thickness of the phase in between the PVF<sub>2</sub> crystalline lamellae of the 40/60 blend remained nearly the same as that of the 50/50 blend, indicating that the additional 10 wt % PBA could be located mainly in interfibrillar and interspherulitic regions, as confirmed by the direct microscopic observation of the crystallization of PBA in the interspherulitic domains of the PVF<sub>2</sub> spherulites and in the interfibrillar pockets of the PVF<sub>2</sub> spherulites for the 40/60 blend.<sup>8</sup> Therefore, the change from the scattering shoulder observed for the 70/30 to 50/50 blends to a scattering peak for the 40/60 blend is presumably due to the strong coherent scattering of PBA crystalline lamellae in the interspherulitic region of the PVF<sub>2</sub> spherulites.

## Conclusions

The results reported in this paper provide new insights into the lamellar organization of the PVF<sub>2</sub>/PBA blends, that go beyond the information previously obtained by differential scanning calorimetry and optical microscopy. It is concluded that the morphology exhibited by the blends depends on the thermal conditions. At temperatures  $T$  such that  $T_m(\text{PVF}_2) > T > T_m(\text{PBA})$ , the blends exist in the semicrystalline/amorphous state, where the PBA component is mainly incorporated in the interlamellar region for the blends containing up to 50 wt % PBA. With increasing PBA content there is apparently a transition from mainly interlamellar inclu-

sion to interlamellar exclusion; this effect is similar to that observed by Cheung *et al.*<sup>6</sup> for PCL/PC blends, for which it was ascribed to the change in the glass transition temperature with blend composition. In the present case, however, that explanation is unlikely because the  $T_g$  of the blends changes only slightly with composition.

For temperatures  $T < T_m(\text{PBA})$  the blends are in the semicrystalline/semicrystalline state, where the crystalline PBA can reside as a thick lamella in the PVF<sub>2</sub> interlamellar region, and there is a mixed amorphous phase between the PBA and PVF<sub>2</sub> lamellae. This mode of lamellar organization is different from that previously proposed by Cheung *et al.*<sup>6</sup> for the semicrystalline/semicrystalline (PC/PCL) blends, where the crystalline lamellae of the two different polymers are mixed in a random fashion.

**Acknowledgment.** B.C. gratefully acknowledges support of this work by the National Science Foundation, Polymers Program (DMR 9301294), the Department of Energy (DE-FG02-86ER45237.012), and the SUNY X3 Beamline at the National Synchrotron Light Source, supported by the Division of Basic Energy Sciences of the U.S. Department of Energy (DE-FG02-86ER45231).

## References and Notes

- (1) Russell, T. P.; Stein, R. S. *J. Polym. Sci., Polym. Phys. Ed.* **1983**, *21*, 999.
- (2) Russell, T. P.; Ito, H.; Wignall, G. D. *Macromolecules* **1988**, *21*, 1703.
- (3) Warner, F. P.; Stein, R. S.; MacKnight, W. J. *J. Polym. Sci., Polym. Phys. Ed.* **1977**, *15*, 2113.
- (4) Keith, H. D.; Padden, F. J. *J. Appl. Phys.* **1964**, *35*, 1270, 1286.
- (5) Cheung, Y. W.; Stein, R. S. *Macromolecules* **1994**, *27*, 2512.
- (6) Cheung, Y. W.; Stein, R. S.; Lin, J. S.; Wignall, G. D. *Macromolecules* **1994**, *27*, 2520.
- (7) Penning, J. P.; Manley, R. St. J. *Macromolecules* **1996**, *29*, 77.
- (8) Penning, J. P.; Manley, R. St. J. *Macromolecules* **1996**, *29*, 84.
- (9) Fujita, K.; Kyu, T.; Manley, R. St. J. *Macromolecules* **1996**, *29*, 91.
- (10) Chu, B.; Harney, P. J.; Li, Y.; Linliu, K.; Yeh, F.; Hsiao, B. S. *Rev. Sci. Instrum.* **1994**, *65*, 597.
- (11) Liu, L.-Z.; Chu, B.; Penning, J. P.; Manley, R. St. J. To be published.
- (12) Strobl, G. R.; Schneider, M. *J. Polym. Sci., Polym. Phys. Ed.* **1980**, *18*, 1343.
- (13) *Small Angle X-ray Scattering*; Glatter, O., Kratky, O., Eds.; Academic Press: London, 1983.
- (14) Ruland, W. *J. Appl. Crystallogr.* **1971**, *4*, 70.
- (15) Deby, P.; Bueche, A. M. *J. Appl. Phys.* **1949**, *20*, 518.
- (16) Cheung, Y. W.; Stein, R. S.; Wignall, G. D.; Yang, H. E. *Macromolecules* **1993**, *26*, 5365.

MA961719N